

## Extracting maximum value from minimal acquisition: A microseismic case study

Ben Witten<sup>1</sup>, Adam M. Baig<sup>1</sup>, Sepi Karimi<sup>1</sup>, Aaron Booterbaugh<sup>1</sup>, Greg Purdue<sup>2</sup>

<sup>1</sup>Nanometrics Inc, <sup>2</sup>Paramount Resources Ltd

### Summary

We present the modelling, acquisition, processing, and results from a light-weight surface microseismic monitoring array. We show that through careful planning, design and processing, it is possible to extract a high-quality microseismic data set from minimum acquisition. This procedure can provide a model of how to optimize monitoring budgets to deliver results for future projects.

We begin by describing the pre-survey modelling and acquisition design process. This takes into account budgetary constraints, desired detection magnitude and location accuracy, and local site conditions. The minimal acceptable design consisted of 15 locations, each containing 7 geophones strings for a total of 630 geophones. This design is substantially smaller than common surface-microseismic monitoring arrays which can have upwards of 20,000 geophones. We briefly discuss the processing procedures for the dataset.

The results of the survey produced over 3700 microseismic events down to  $M_w = -1.79$ . The final catalog provides an interpretable data set of the seismicity which changes across the pad, reflecting inhomogeneities in the subsurface geology and engineering parameters. In particular, we, counter-intuitively, observe microseismic events trend away from a depleted zone.

### Pre-survey modelling

Prior to monitoring the project, we perform modelling to design the minimal array to meet operators objectives. The primary design parameter was to construct an array capable of detecting and locating all microseismic events with a moment magnitude ( $M_w$ ) greater than -1.0 (i.e. magnitude of completeness [Mc] is -1.0) with lowest possible channel count. The inputs to the modelling were the well path, velocity model, Q, surface noise level, and source parameters. Using this information, we model synthetic events into various array designs. Then, following the processing procedure described in the subsequent section, we attempt to detect and locate events of different magnitudes. To better approximate field conditions, station statics are applied to account for velocity errors. Table 1 shows the assumptions for this modelling.

The tested array designs consisted of superstations (Witten, et al. 2019), which are small patch arrays. Each superstation is constructed from a series of hexagonal rings. Figure 1 shows an

example superstation with 3 hexagonal rings. Each triangle represents a node consisting of a string of 6 geophones.

Given the high noise assumption of -104 dB, 15 superstations

Table 1. Assumptions for detectability modeling.

Parameter	Value
Source depth	3150 m
Source mechanism	Strike-slip
Source static stress drop	0.3 MPa
Attenuation (Q)	60
Velocity error (as static shifts) for imaging approach	3 ms
Average noise level	Range from -114 dB to -104 dB

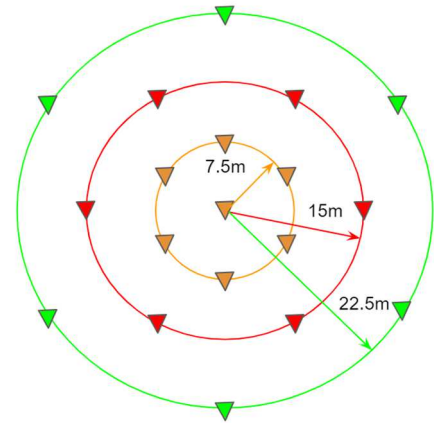
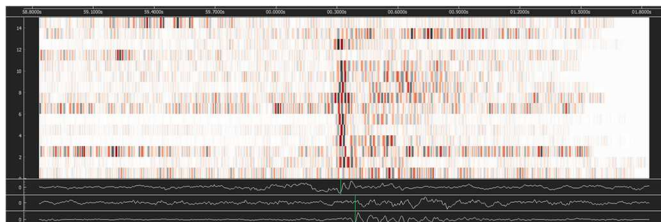


Figure 1. Example superstation design with 3 hexagonal rings. Each triangle

with 7 nodes each, the orange locations in Figure 1, provided an Mc of -1.06, satisfying the monitoring objectives. Therefore, the array has a total of 105 locations of 6-geophone strings for a total of 630 geophones.

## Processing methodology

The processing consists of noise attenuation, initial event detection, velocity updating, event detection/location, magnitude calculation and moment tensor inversion. The steps of the noise attenuation include time-frequency despiking to remove statistical outliers, bandpass filtering, and semblance-weighted stacking within each superstation (Chambers, 2018). Using initially detected events, we update the velocity model, including VTI parameters, through particle swarm optimization (PSO) (Shaw and Srivastava, 2007).



We apply an imaging-based joint event detection/location algorithm to move-out and stack the superstation data similar to Kao and Shan (2004). Each potential detection is manually quality controlled (QC) to ensure only true positives are further analyzed and delivered. Figure 2 shows an example QC view for a true event with data aligned based on the optimal location.

We calculate moment magnitudes for each event in the catalog through a fitting procedure (Baig, et al 2019). In addition, we invert for moment tensors (MT) for each event and for a noise window prior to each event. The noise MTs provide statistical confidence value for each event MT solution. See Baig et al. (2020) for more details.

## Results and Interpretation

A total of 3759 events were located during the 5-well, 295-stage fracture program, with a magnitude range from -1.79 to 0.59 with a  $M_c$  of -1.0. The results matched the pre-survey modelling and met the monitoring objectives. Figure 3 shows the event locations colored by time. The expected signature of microseismicity following fluid into the depleted zone (the area between wells 3 and 4 towards the heel) was not observed. In fact, this zone was notable for its lack of seismicity.

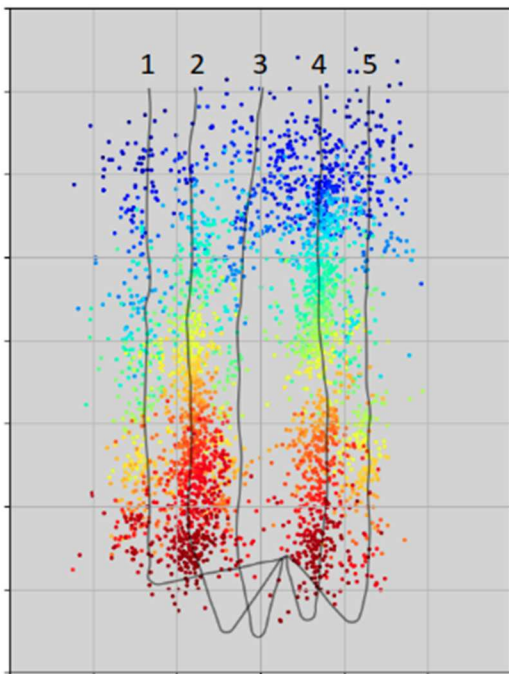


Figure 3. Event locations colored by time.

To further understand the seismicity, we cluster the moment tensor results based on mechanism similarity. From these clusters, we observe, the areas around the depletion zone have less normal mechanisms components (Figure 4). Further results from stress inversion analysis show that in these areas, the most tensional stress axis ( $\sigma_3$ ) moves to relatively low values. Towards the toe of well 4, the stress regime trends to more normal, indicating a relative increase of vertical stresses reflected in the stress inversions. Our results suggest that the seismically quiet region of previously-fractured reservoir does not have the strength to generate seismicity, but acts as a conduit to extend fractures around it.

## Conclusions

We demonstrate a workflow to design, process and interpret a microseismic acquisition program. This workflow strives to extract the most amount of information from a minimal array design. The goal is to provide a sufficient data set to make interpretations

of the resulting fracture program without the need for an extremely large field program. The procedure provides a blueprint for turn-key microseismic acquisition design, careful processing and quality control. The presented results demonstrate a proof-of-concept that a light-weight monitoring array can achieve interpretable results and meet predefined objectives.

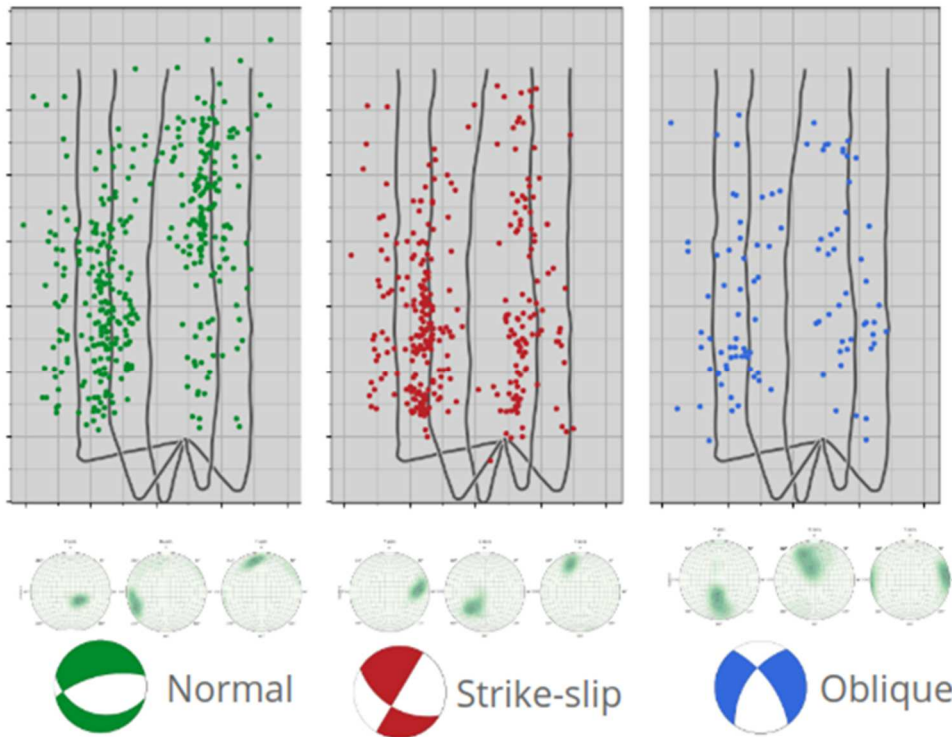


Figure 4. Event locations colored by moment tensor solution cluster. The average mechanism for each cluster is shown.

## Acknowledgements

We thank Paramount Resources, Chevron Canada Limited and KUFPEC Canada for permission to publish this work.

## References

Baig, A., B. Witten, S. Karimi, D. Baturan, and E. Yenier, (2019), Magnitude calibration of imaging-based microseismic locations, *SEG Technical Program Expanded Abstracts* : 3086-3090.

Baig, A., B. Witten, and S. Karimi, (2020), Quality Control of Microseismic Moment Tensors from Surface-Based Acquisitions, *Geoconvention*, submitted.

Chambers, K. (2018), Noise attenuation in sparse-surface microseismic datasets, *SEG Technical Program Expanded Abstracts* : 2902-2906.

Kao, H., and S.-J. Shan (2004). The Source-Scanning Algorithm: mapping the distribution of seismic sources in time and space, *Geophys. J. Int.*, 157, 589-594.

Shaw, R. and S. Srivastava, (2007), Particle swarm optimization: A new tool to invert geophysical data, *GEOPHYSICS* 72: F75-F83.

Witten, B., A. Booterbaugh, and R. Segstro, (2019), "A novel array acquisition and processing methodology for microseismic monitoring": *EAGE Conference Proceedings*, 81st Conference and Exhibition.

*GeoConvention 2020*